PharmacoEconomics (2024) 42:231–247
https://doi.org/10.1007/s40273-023-01322-2

ORIGINAL RESEARCH ARTICLE

Cost-Effectiveness Modeling of Prostate-Specific Membrane Antigen Positron Emission Tomography with Piflufolastat F 18 for the Initial Diagnosis of Patients with Prostate Cancer in the United States

Christopher W. Yee[1] · Michael J. Harvey[1] · Yiqiao Xin[1] · Noam Y. Kirson[1]

Accepted: 1 October 2023 / Published online: 7 November 2023

Abstract

Background and objectives Piflufolastat F 18 is a novel prostate-specific membrane antigen (PSMA)-targeted positron emission tomography (PET) radiotracer that is superior to standard of care (SOC) imaging for the initial staging of prostate cancer and the detection of biochemical recurrence. As piflufolastat F 18 has been approved in the United States (US) for this indication, this modeling study assessed the cost effectiveness of piflufolastat F 18 versus fluciclovine F-18, gallium68-PSMA-11 (PSMA 11), and SOC imaging (a mix of bone scans, computed tomography, and magnetic resonance imaging) for the diagnosis and staging of prostate cancer from a US healthcare system perspective.

Perspective A US third-party payer perspective was used, which for this population reflects a mix of commercial and Medicare, considering only direct healthcare costs.

Setting This study utilized a tertiary healthcare setting.

Methods A decision tree was used to map the diagnostic/treatment pathway, consisting of the proportion of patients with local, regional, distant, or no disease; prostate-specific antigen (PSA) ≤ 1.0 or > 1.0; and accuracy of imaging modalities. A Markov model predicted the long-term outcomes of disease progression according to treatment decisions. Inputs to the model were informed by data from the OSPREY and CONDOR clinical trials, public data, and the literature. Treatment mix included active surveillance, radiation therapy, prostatectomy, androgen deprivation therapy (ADT), and radiation therapy + ADT, informed by expert opinion. Outcomes included life-years (LY), quality-adjusted life-years (QALY), and the incremental cost-effectiveness ratio (ICER). All costs were reported in 2021 US dollars, using the US Bureau of Labor Statistics Consumer Price Index. A willingness-to-pay (WTP) threshold of $150,000 was considered cost effective, consistent with the upper range used as the standard for price benchmarks by the Institute for Clinical and Economic Review. The robustness of the base-case results was assessed in deterministic and probabilistic sensitivity analyses.

Results Over a lifetime horizon, piflufolastat F 18 had the greatest effectiveness in terms of LYs (6.80) and QALYs (5.33); for the comparators, LYs ranged from 6.58 (SOC) to 6.76 (PSMA 11) and QALYs ranged from 5.12 (SOC) and 5.30 (PSMA 11). Piflufolastat F 18 was more cost effective compared with fluciclovine F 18, PSMA 11, and SOC, with ICERs of $21,122, $55,836, and $124,330 per QALY gained, respectively. Piflufolastat F 18 was associated with the greatest net monetary benefit ($627,918) compared with the other options at a WTP threshold of $150,000. The results of the deterministic and probabilistic sensitivity analyses supported the robustness of the base-case results.

Conclusions This study suggests that piflufolastat F 18 is a cost-effective diagnostic option for men with prostate cancer in the US, with higher associated LY, QALY, and greater net monetary benefit than fluciclovine F 18, PSMA 11, and SOC imaging.

1 Introduction

Prostate cancer is the most common non-cutaneous cancer in men, affecting approximately 3.3 million men in the United States (US) in 2019 [1, 2]. An estimated 268,490 new prostate cancer cases will occur in the US during 2022, representing 27% of new cancer diagnoses in men and 14.0% of all new cancer cases [1–3]. The 5-year relative survival across all stages of prostate cancer is high (96.8%), driven by individuals with localized or regional disease, but sharply decreases among those with metastatic (i.e., distant) disease (32.3%) [2, 3]. Additionally, up to 50% of patients with localized prostate cancer experience biochemical recurrence (BCR)—an increase in serum levels of prostate-specific antigen (PSA)—within 10 years following radical prostatectomy

Extended author information available on the last page of the article

Key Points for Decision Makers

Piflufolastat F 18 is a novel prostate-specific membrane antigen (PSMA)-targeted positron emission tomography radiotracer that was recently approved in the United States for men with prostate cancer and suspected metastasis who are candidates for initial definitive therapy, or with suspected biochemical recurrence.

This study assessed the cost effectiveness of piflufolastat F 18 in the US compared with other imaging modalities for prostate cancer, including fluciclovine F-18, gallium68-PSMA-11 (PSMA 11), and standard of care imaging (a mix of bone scans, computed tomography, and magnetic resonance imaging) for the diagnosis and staging of prostate cancer.

Our analysis suggests that piflufolastat F 18 is a cost-effective diagnostic option for prostate cancer in the US when using a willingness-to-pay threshold of US$150,000, and that it was associated with greater life-years, quality-adjusted life-years, and net monetary benefit than the comparators.

or radiation therapy [4, 5], and BCR often precedes metastases [6].

The diagnostic workup of prostate cancer typically involves digital rectal exam, serological PSA testing, and ultrasound-guided biopsy [1, 6]. If a prostate cancer diagnosis is confirmed, imaging may then be used to define the extent of local disease or presence of nodal and distant metastases [1]. However, conventional imaging methods such as computed tomography (CT), magnetic resonance imaging (MRI), positron emission tomography (PET) with 18F-fluorodeoxyglucose (18F-FDG), and bone scans are inadequate for detecting metastatic or recurrent disease [1, 7–9]. Recently, the use of novel PET modalities for imaging prostate cancer has garnered increasing interest owing to its ability to detect metastases with high sensitivity and specificity [7]. Multiple PET radiotracers have been developed, including those targeting tumor metabolism (e.g., fluciclovine F 18, also known as 18F-FACBC, and 11C/18F-choline) and prostate-specific membrane antigen (PSMA; e.g., gallium68-PSMA-11 [PSMA 11], also known as 68Ga-PSMA-11, and piflufolastat F 18, also known as 18F-DCFPyL) [7, 10].

Advanced imaging could facilitate more accurate localization and staging of prostate cancer, which may in turn result in better treatment decisions and, consequently, patient outcomes. For optimal prostate cancer management, it is crucial to rule out metastasis in patients diagnosed with localized disease prior to the implementation of definitive local therapies. An inaccurate or delayed diagnosis may lead to unnecessary treatment for truly indolent disease or a missed opportunity for providing appropriate interventions for aggressive disease [7]. Furthermore, the ability to determine whether a rise in PSA is due to local or widely metastatic recurrence is also essential for the identification of patients with localized or oligometastatic disease who may still benefit from curative salvage radiotherapy [11–13].

PSMA PET is recognized in prostate cancer management guidelines as a sensitive and specific technique for detecting metastasis [1, 8, 12, 14]. Specifically, the CONDOR trial of the PSMA-targeted PET radiotracer piflufolastat F 18 demonstrated that incorporation of PET imaging results led to changes to management plans in 64% of patients with prostate cancer and BCR [15, 16]. Results from the phase II/III OSPREY trial indicated that piflufolastat F 18 imaging during the initial staging of patients with high-risk prostate cancer was superior to standard of care (SOC) imaging, allowing clinicians to optimize treatment from the beginning of care [17]. In OSPREY, the positive predictive value of piflufolastat F 18 for detecting extra-prostatic lesions was 86.7% for high-risk patients and 83.2% for patients with suspected recurrent/metastatic disease [18]. These results led to the approval of piflufolastat F 18 by the US Food and Drug Administration (FDA) in May 2021 as a PSMA PET agent for patients with suspected prostate cancer metastasis who are candidates for initial definitive therapy or with suspected prostate cancer recurrence based on elevated serum PSA levels [10].

Given the FDA approval of piflufolastat F 18, and its potential to improve prostate cancer management and clinical benefit, healthcare payers and providers would be interested to understand the economic and clinical value of incorporating it in the prostate cancer care pathway, both at initial staging and for detection and localization of BCR disease. In addition, due to the longer half-life and higher cyclotron production rates of F-18 compared with Ga-68, F-18 products can be produced in greater quantity and in more centralized locations than Ga-68 products. This enables several efficiency advantages in the manufacture and distribution of F-18 products over Ga-68 products to deliver the same number of patient doses, including (1) fewer cyclotron run hours, (2) fewer batches of product to be prepared, (3) fewer dose preparation locations and personnel, and (4) fewer drivers and miles to deliver doses within a given geography. Cost-effectiveness analysis can provide evidence to inform coverage and treatment decisions; however, no such analysis has been conducted for piflufolastat F 18. Therefore, this study aimed to assess the cost effectiveness of piflufolastat F 18 compared with alternative diagnostic imaging modalities

(fluciclovine F-18, PSMA 11, and SOC imaging—a mix of bone, CT, and MRI scans) for the staging of prostate cancer in a starting patient population of newly diagnosed patients with local or regional prostate cancer, of whom a subset will go on to experience BCR, from a US healthcare system perspective; specifically, from the perspective of third-party payers, which for this population reflects a mix of commercial and Medicare, with only direct healthcare costs considered.

2 Methods

2.1 Model Structure

An economic evaluation was conducted using a hybrid model structure consisting of (1) a decision tree to map the clinical diagnostic and treatment pathway, consisting of the proportion of patients with local, regional, distant, or no disease; PSA ≤ 1.0 or > 1.0; and testing accuracy of the imaging modalities; and (2) a Markov model to predict the long-term outcomes of disease progression associated with the different treatment decisions (Fig. 1). The analysis was conducted from a US payer's perspective over a lifetime horizon; the population reflects a mix of commercial and Medicare payers. Two time points were considered: initial diagnosis and BCR. Separate sets of inputs for the distribution of PSA levels (> 1.0 vs ≤ 1.0) and disease states (e.g., local, regional) were obtained for each time point, which in turn affected the detection rates (i.e., inputs corresponded to PSA levels) and treatment effectiveness (i.e., inputs corresponded to transitions between disease states) at each time point (Tables 1, 2, 3). This is in accordance with findings that sensitivity and specificity differ between PSA levels, disease states, and time points [19]. The use of piflufolastat F 18 among patients for the initial staging and diagnosis of prostate cancer, as well as the detection and staging of recurrent prostate cancer, was modeled. The imaging modalities compared with piflufolastat F 18 were fluciclovine F 18, PSMA 11, and SOC imaging (MRI, bone scan, and CT [equally weighted]). A half-cycle correction was applied in the model to the proportions of patients in each disease state; costs and utilities were applied to these adjusted proportions and did not have a separate half-cycle correction.

2.2 Decision Tree

The decision tree captured the diagnostic pathway and was first separated by true disease status, including local, regional, distant, or no prostate cancer (Fig. 1a). Within each disease status, patients were stratified by PSA level $\leq$ or > 1.0 due to different imaging test performance in these groups. Alternative diagnostic outcomes were assigned probabilities based on true disease status. For example, if the true disease status was local prostate cancer, the decision tree predicted the number of individuals who would be correctly confirmed as having local prostate cancer (true positive) or incorrectly found to have no prostate cancer (false negative). In contrast, if the true disease status was no prostate cancer, the decision tree predicted the number of individuals who would be correctly confirmed as having no prostate cancer (true negative) or incorrectly found to have prostate cancer (false positive). Patients with each type of diagnosis were assigned to different treatment strategies. In particular, patients with a false negative or a false positive were treated for a 12-month period according to the disease state they were falsely assumed to be in (e.g., false-negative patients with distant disease were treated as if they had regional disease; false negative patients with regional disease were treated as if they had local disease, and false negative patients with local disease were treated as if they had no disease), after which they received treatment appropriate to their true disease state without incurring additional diagnostic costs.

2.3 Markov Model

The Markov model tracked the transition of patients with the assigned treatment strategies based on their diagnosis, and simulated patients' progression through various states of prostate cancer until death. Patients were categorized into and transitioned through the following health states: no prostate cancer (only for recurrence diagnosis), local, regional, and distant prostate cancer. The transitions were modeled over monthly cycles, and healthcare costs and outcomes of prostate cancer management are accumulated over a lifetime horizon. All-cause and prostate cancer-specific mortality was also modeled. After a patient had been diagnosed with prostate cancer, they would be treated with a designated therapy based on the decision tree which would impact their progression through the model from their initial health state. Transition probabilities across states were dependent upon the diagnostic pathways and the resulting treatment decisions made at the end of the decision tree.

2.4 Key Assumptions

Several key assumptions were included in the model. First, the distribution of health states and the distribution of PSA level by disease localization did not change by diagnostic method used. Second, test performance (sensitivity and specificity) was assumed not to vary by disease localization. Patients with more than one localization (e.g., lymph node-positive [N1M1]) were classified as the more severe case. Third, patients were assigned treatment based on test results. For true positives and true negatives, costs and QALYs

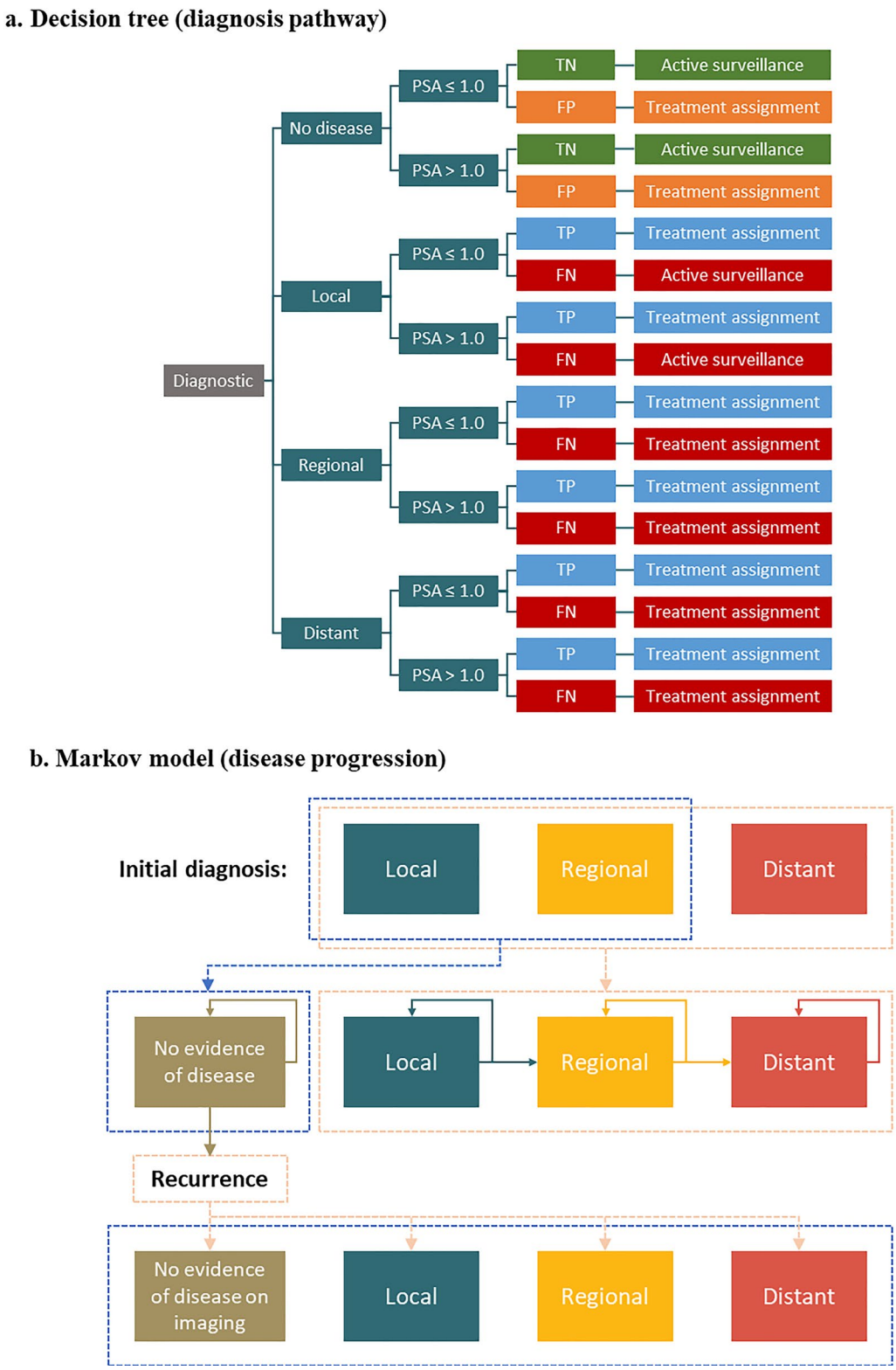

Fig. 1 Model schema. *FN* false negative, *FP* false positive, *PSA* prostate-specific antigen, *TN* true negative, *TP* true positive

Table 1 Key model inputs in the decision tree for the base case and PSA

	Value	Source
Disease state distribution (%)		
Initial diagnosis		
No disease	0	OSPREY 2301[a] [20]
Local	74.20	OSPREY 2301[a] [20]
Regional	25.80	OSPREY 2301[a] [20]
Distant	0.00	OSPREY 2301[a] [20]
Recurrence diagnosis		
No evidence of disease on imaging	0	CONDOR 3301[a] [21]
Local	27.00	CONDOR 3301[a] [21]
Regional	30.00	CONDOR 3301[a] [21]
Distant	43.00	CONDOR 3301[a] [21]
PSA distribution (%)		
Initial diagnosis		
No disease—≤ 1.0	0.00	OSPREY 2301[a] [20]
No disease—> 1.0	100.00	OSPREY 2301[a] [20]
Local—≤ 1.0	0.00	OSPREY 2301[a] [20]
Local—> 1.0	100.00	OSPREY 2301[a] [20]
Regional—≤ 1.0	0.00	OSPREY 2301[a] [20]
Regional—> 1.0	100.00	OSPREY 2301[a] [20]
Distant—≤ 1.0	0.00	OSPREY 2301[a] [20]
Distant—> 1.0	100.00	OSPREY 2301[a] [20]
Recurrence diagnosis		
No disease—≤ 1.0	75.00	CONDOR 3301[a] [21]
No disease—> 1.0	25.00	CONDOR 3301[a] [21]
Local—≤ 1.0	34.50	CONDOR 3301[a] [21]
Local—> 1.0	65.50	CONDOR 3301[a] [21]
Regional—≤ 1.0	42.90	CONDOR 3301[a] [21]
Regional—> 1.0	57.10	CONDOR 3301[a] [21]
Distant—≤ 1.0	20.80	CONDOR 3301[a] [21]
Distant—> 1.0	79.20	CONDOR 3301[a] [21]
Treatment assignment (%)		
Initial diagnosis		
No disease—active surveillance	100.00	Expert opinion
Local—radiation therapy	45.00	Expert opinion
Local—prostatectomy	55.00	Expert opinion
Regional—radiation therapy + ADT	100.00	Expert opinion
Distant—ADT	100.00	Expert opinion
Recurrence diagnosis		
No evidence of disease on imaging—active surveillance	100.00	Assumption
Local—radiation therapy	30	Jensen et al. 2020 [22]
Local—ADT	35	Jensen et al. 2020 [22]
Local—prostatectomy	5	Jensen et al. 2020 [22]
Local—cryotherapy	5	Jensen et al. 2020 [22]
Local—radiation therapy + ADT	25	Jensen et al. 2020 [22]
Regional—radiation therapy	20	Jensen et al. 2020 [22]
Regional—ADT	45	Jensen et al. 2020 [22]
Regional—cryotherapy	5	Jensen et al. 2020 [22]
Regional—radiation therapy + ADT	30	Jensen et al. 2020 [22]
Distant—radiation therapy	30	Jensen et al. 2020 [22]
Distant—ADT	45	Jensen et al. 2020 [22]

Table 1 (continued)

	Value	Source
Distant—radiation therapy + ADT	25	Jensen et al. 2020 [22]
Costs (USD)		
Piflufolastat F 18	6274.17	CMS & Micromedex RED BOOK[b] [41, 42]
Fluciclovine F 18	6336.17	CMS & Micromedex RED BOOK[b] [41, 42]
PSMA 11	6036.17	CMS & Micromedex RED BOOK[b] [41, 42]
MRI	483.10	CMS [41]
SPECT	1385.63	CMS [41]
CT	241.90	CMS [41]

Costs are presented in 2021 US dollars

ADT androgen deprivation therapy, *CMS* Centers for Medicare & Medicaid Services, *CT* computed tomography, *MRI* magnetic resonance imaging, *PET* positron emission tomography, *PSA* prostate-specific antigen, *PSMA* prostate-specific membrane antigen, *SPECT* single-photon emission computerized tomography, *USD* United States dollars

[a]Data on file, Lantheus

[b]Costs listed for each radiotracer include a facility payment amount of $1536.17 for PET, sourced from CMS, added to the average wholesale price of each radiotracer, sourced from Micromedex RED BOOK

were applied as appropriate. For false negatives (only for patients with actual disease), the costs for the lower stage of diagnosis and QALYs for no treatment at the current stage were applied. This assumed the patient was under-staged, so costs were applied but the QALYs reflected the worst case. For false positives (only for patients without disease), costs for the treatment of local disease were applied and QALYs for no disease were applied. This assumed that patients received unnecessary treatment costs and no benefit from treatment. Fourth, an incorrect diagnosis period of 12 months was assumed. Fifth, skipping states was not permitted in the Markov model (e.g., no path from local to distant), as data were not available to model these transitions. Sixth, as a simplifying assumption, BCR could only occur once in the model. Likewise, retesting following an incorrect diagnosis was not modeled (see Sect. 2.2). Lastly, prostate cancer-associated death could only be reached from the distant disease state.

2.5 Key Model Inputs

Model inputs were obtained through a targeted literature review using PubMed. Search terms included 'prostate cancer' for prostate cancer-specific inputs; the various terms for the specific radiotracers for testing accuracy inputs (e.g., for PSMA 11, including both 'gallium68-PSMA-11' and '68Ga-PSMA-11'); and 'price,' 'cost,' 'utility,' and 'quality of life' for cost and utility inputs, respectively. For clinical parameters, standalone studies, particularly randomized clinical trials, with higher sample sizes were preferred. For healthcare costs, US claims-based studies were preferred. For utilities, studies in a US setting, which provided a more complete set of utilities, were preferred.

2.5.1 Clinical Parameters

In the decision tree, clinical parameters included test performance stratified by PSA, disease state distribution, PSA distribution, and treatment assigned, as informed by clinical trials (see inputs listed in Table 1). Disease state distribution and PSA distribution probabilities were based on clinical study reports from the OSPREY and CONDOR clinical trials for piflufolastat F 18, which reported the PSA levels at baseline for each cohort [20, 21]. Inputs for treatment assignments at initial diagnosis were based on expert opinion—proportions were elicited during targeted one-on-one interviews with clinicians (see Acknowledgements). Treatment assignment at recurrence diagnosis was based on inputs for an economic model of fluciclovine F 18 for the staging of recurrent prostate cancer in the US, which retrospectively analyzed treatment plans for patients from the LOCATE (Localizing Occult prostate Cancer metastases with Advanced imaging TEchniques) trial (ClinicalTrials.gov identifier: NCT02680041), an open-label, multicenter interventional trial for patients with BCR [22, 23].

In the Markov model, clinical parameters included transition (i.e., progression) probabilities, adverse event (AE) probabilities, and treatment efficacy, including the probability of cure at initial diagnosis (see inputs listed in Table 2). State transition probabilities were based on inputs for a microsimulation and a Markov model that each modeled the progression of prostate cancer, validated against data from the European Randomized Study of Screening for Prostate Cancer (ERSPC) and Surveillance Epidemiology End Results (SEER) data, respectively [24–28]. Probabilities of erectile dysfunction in radiation therapy, prostatectomy, and radiation therapy + androgen deprivation therapy (ADT), along with the probability of

Table 2 Key model inputs in the Markov model for the base case and probabilistic sensitivity analysis

	Value	Source
State transition probabilities (%)		
No disease to local (initial diagnosis)	9.70	Draisma et al. 2003 [27]
No disease to local (recurrence diagnosis)	5.60	Cowen et al. 1994 [24]
Local to regional	12.70	Cowen et al. 1994 [24]
Regional to distant	34.00	Cowen et al. 1994 [24]
Distant to death (prostate cancer-related)	26.00	Cowen et al. 1994 [24]
Probabilities of adverse events (%)		
Erectile dysfunction in radiation therapy	27.00	Cooperberg et al. 2013 [29]
Erectile dysfunction in ADT	10.00	Sciarra et al. 2016 [30]
Erectile dysfunction in prostatectomy	42.00	Cooperberg et al. 2013 [29]
Erectile dysfunction in cryotherapy	27.00	Zhou et al. 2019 [31]
Erectile dysfunction in radiation therapy + ADT	27.00	Cooperberg et al. 2013 [29]
Urinary incontinence in prostatectomy	9.00	Cooperberg et al. 2013 [29]
Urinary incontinence in cryotherapy	10.00	Roberts et al. 2011 [32]
Treatment effectiveness on transition probabilities (%)		
Local to regional		
Active surveillance	1.00	Assumption
Radiation therapy	0.27	Trock et al. 2008 [33]
ADT	0.37	Bauman et al. 2020 [34]
Prostatectomy	0.34	Chade et al. 2011 [35]
Cryotherapy	0.31	Bauman et al. 2020 [34]
Radiation therapy + ADT	0.36	Trock et al. 2008 [33]
Regional to distant		
Active surveillance	1.00	Assumption
Radiation therapy	0.54	Trock et al. 2008 [33]
ADT	0.64	Bauman et al. 2020 [34]
Prostatectomy	0.61	Chade et al. 2011 [35]
Cryotherapy	0.59	Bauman et al. 2020 [34]
Radiation therapy + ADT	0.63	Trock et al. 2008 [33]
Distant to death		
Active surveillance	1.00	Assumption
Radiation therapy	0.80	Trock et al. 2008 [33]
ADT	0.86	Bauman et al. 2020 [34]
Prostatectomy	0.84	Chade et al. 2011 [35]
Cryotherapy	0.83	Bauman et al. 2020 [34]
Radiation therapy + ADT	0.85	Trock et al. 2008 [33]
Costs (USD)		
Treatment costs		
Active surveillance (Year 1)	1329.51	Jensen et al. 2020 [22]
Active surveillance (Year ≥ 2)	822.56	Jensen et al. 2020 [22]
Radiation therapy (Year 1)	2426.32	Jensen et al. 2020 [22]
Radiation therapy (Year ≥ 2)	413.07	Jensen et al. 2020 [22]
ADT (Year 1)	1492.47	Jensen et al. 2020 [22]
ADT (Year ≥ 2)	990.42	Jensen et al. 2020 [22]
Prostatectomy (Year 1)	11,049.93	Jensen et al. 2020 [22]
Prostatectomy (Year ≥ 2)	0.00	Jensen et al. 2020 [22]
Cryotherapy (Year 1)	6540.70	Jensen et al. 2020 [22]
Cryotherapy (Year ≥ 2)	0.00	Jensen et al. 2020 [22]
Radiation therapy + ADT (Year 1)	3172.50	Jensen et al. 2020 [22]
Radiation therapy + ADT (Year ≥ 2)	587.63	Jensen et al. 2020 [22]

Table 2 (continued)

	Value	Source
AE costs		
Erectile dysfunction (Year 1)	162.42	Cooperberg et al. 2013 [29]
Erectile dysfunction (Year ≥ 2)	58.08	Cooperberg et al. 2013 [29]
Urinary incontinence (Year 1)	108.92	Cooperberg et al. 2013 [29]
Urinary incontinence (Year ≥ 2)	65.00	Cooperberg et al. 2013 [29]
Medical costs		
HRU (Local)	2746.00	Appukkuttan et al. 2020 [44], Tangirala et al. 2019 [45]
HRU (Regional)	3295.20	Appukkuttan et al. 2020 [44], Tangirala et al. 2019 [45]
HRU (Distant)	5784.58	Appukkuttan et al. et al.
Utilities		
No disease	0.90	Jiang et al. 2021 [48]
Local disease	0.79	Stewart et al. 2005 [50]
Regional disease	0.67	Stewart et al. 2005 [50]
Distant disease	0.25	Stewart et al. 2005 [50]
Death (prostate cancer-related)	0.00	Assumption
Death (other causes)	0.00	Assumption
Erectile dysfunction	− 0.10	Cooperberg et al. 2013 [29]
Urinary incontinence	− 0.20	Cooperberg et al. 2013 [29]
Incorrect diagnosis period		
Incorrect diagnosis period (months)	12.00	Assumption
Probabilities of cure after initial diagnosis (%)		
Active surveillance in all states	0	Expert opinion
All active treatment for local disease	90	Expert opinion
All active treatment for regional disease	80	Expert opinion
All active treatment for distant disease	0	Expert opinion
Probabilities of recurrence from cure of initial disease		
Recurrence from cure of initial local disease	6.89	Expert opinion
Recurrence from cure of initial regional disease	16.74	Expert opinion

Costs are presented in 2021 USD

ADT androgen deprivation therapy, *AE* adverse event, *HRU* healthcare resource utilization, *USD* United States dollars

urinary incontinence in prostatectomy, were based on a cost-utility analysis of treatments for localized prostate cancer from a US payer perspective [29]. Probabilities of erectile function in ADT and cryotherapy were based on meta-analyses for these two respective treatments, while the probability of urinary incontinence in cryotherapy was based on a population-based study of men diagnosed with localized prostate cancer in a SEER-Medicare-linked database [30–32]. The treatment effectiveness of radiation therapy and radiation therapy + ADT was based on a retrospective cohort analysis of men undergoing prostatectomy who received salvage treatment with either radiation therapy alone or radiation therapy + ADT [33]. Treatment effectiveness of ADT and cryotherapy was based on a propensity score-matched analysis of men with prostate cancer treated with either ADT or cryotherapy [34]. The treatment effectiveness of prostatectomy was based on a multi-center study of men with radiation-recurrent prostate cancer treated with salvage radical prostatectomy [35]. Probabilities of cure at initial diagnosis, and of recurrence from cure of initial disease, were based on expert opinion, and elicited from one-on-one interviews with clinicians (see Acknowledgements).

The model inputs for diagnostic test performance (i.e., sensitivity and specificity) by PSA level (i.e., ≤ 1.0 or > 1.0) are detailed in Table 3. The sensitivities and specificities of piflufolastat F 18 were based on clinical study reports from the OSPREY clinical trial [20]. The sensitivities of

Table 3 Test performance inputs in populations with different PSA levels

	%	Source
Piflufolastat F 18		
Sensitivity—PSA ≤ 1.0	57.00	OSPREY 2301[a] [20]
Sensitivity—PSA > 1.0	97.00	OSPREY 2301[a] [20]
Specificity—PSA ≤ 1.0	93.00	OSPREY 2301[a] [20]
Specificity—PSA > 1.0	55.00	OSPREY 2301[a] [20]
Fluciclovine F 18		
Sensitivity—PSA ≤ 1.0	30.00	Scarsbrook et al. 2020 [36]
Sensitivity—PSA > 1.0	85.00	Scarsbrook et al. 2020 [36]
Specificity—PSA ≤ 1.0	67.00	Bach-Gansmo et al. 2017 [37]
Specificity—PSA > 1.0	31.00	Bach-Gansmo et al. 2017 [37]
PSMA 11		
Sensitivity—PSA ≤ 1.0	41.00	Asokendaran et al. 2019 [38]
Sensitivity—PSA > 1.0	92.00	Asokendaran et al. 2019 [38]
Specificity—PSA ≤ 1.0	67.00	Expert opinion (same as fluciclovine F 18)
Specificity—PSA > 1.0	89.00	Li et al. 2020 [40]
MRI		
Sensitivity—PSA ≤ 1.0	18.00	Expert opinion (same as CT)
Sensitivity—PSA > 1.0	68.00	Expert opinion (+5% above CT)
Specificity—PSA ≤ 1.0	67.00	Expert opinion (same as fluciclovine F 18)
Specificity—PSA > 1.0	53.00	Li et al. 2020 [40]
SPECT		
Sensitivity—PSA ≤ 1.0	10.00	de Leiris et al. 2020 [39]
Sensitivity—PSA > 1.0	25.00	de Leiris et al. 2020 [39]
Specificity—PSA ≤ 1.0	67.00	Expert opinion (same as fluciclovine F 18)
Specificity—PSA > 1.0	31.00	Expert opinion (same as fluciclovine F 18)
CT		
Sensitivity—PSA ≤ 1.0	18.00	Asokendaran et al. 2019 [38]
Sensitivity—PSA > 1.0	63.00	Asokendaran et al. 2019 [38]
Specificity—PSA ≤ 1.0	67.00	Expert opinion (same as fluciclovine F 18)
Specificity—PSA > 1.0	31.00	Expert opinion (same as fluciclovine F 18)

CT computed tomography, *MRI* magnetic resonance imaging, *PSA* prostate-specific antigen, *PSMA* prostate-specific membrane antigen, *SPECT* single-photon emission computerized tomography

[a]Data on file, Lantheus

fluciclovine F 18 were based on results from the FALCON trial of fluciclovine F 18 in men with BCR, while the specificities were based on results from the BED-001 study of patients who received at least one injection of fluciclovine F 18 for the detection of BCR [36, 37]. The sensitivities of PSMA 11 and CT were based on a retrospective single-site clinical audit comparing gallium68-PSMA PET/CT and standard CT imaging in patients with a rising PSA after definitive treatment for prostate cancer [38]. The sensitivities of SPECT were based on a single-center retrospective study comparing SPECT and F 18-choline PET/CT imaging in prostate cancer patients initially referred for F 18-choline PET/CT [39]. The specificities of PSMA 11 and MRI for PSA > 1.0 were based on a study that compared gallium68-PSMA-617 PET/CT and MRI in patients with suspected prostate cancer [40]. The sensitivity of MRI for PSA ≤ 1.0 was assumed to be the same as CT, while for PSA > 1.0 it was assumed to be + 5% above CT. The specificities of PSMA 11, MRI, SPECT, and CT for PSA ≤ 1.0 were assumed to be the same as fluciclovine F 18.

2.5.2 Healthcare Costs

Healthcare cost categories included diagnostic strategies, prostate cancer treatment, and AE management (Tables 1 and 2). Costs per procedure for all imaging modalities (i.e., piflufolastat F 18, fluciclovine F 18, PSMA 11, MRI, SPECT, and CT) were based on Centers for Medicare & Medicaid Services (CMS) physician fee schedules and Average Wholesale Price Micromedex RED BOOK [41, 42]. Treatment costs for prostate cancer were based on inputs for an economic model of fluciclovine F 18 for the staging of

recurrent prostate cancer in the US, which used claims from the Limited Data Set (LDS) comprised of a random sample of all Medicare claims that have fee-for-service coverage [22, 43]. AE costs for erectile dysfunction and urinary incontinence were based on a cost-utility analysis of treatments for localized prostate cancer from a US payer perspective [29]. Medical costs arising from healthcare resource utilization were based on claims studies using the Truven Health Analytics MarketScan® Commercial Claims and Encounters and Truven Health Analytics MarketScan® Medicare Supplemental and Coordination of Benefits database; along with the Premier Healthcare Database, a US hospital-based, all-payer database [44, 45]. All costs were reported in 2021 US dollars (USD) and discounted at 3% annually, in accordance with guidance for US-based studies [46]. Where required, the US Bureau of Labor Statistics Consumer Price Index for medical care services was used to inflate costs to 2021 values [47].

2.5.3 QALYs

In the estimation of QALYs, utilities were considered at each Markov model state; disutility related to AEs was also considered. The utility of having no disease was based on a study of US population norms elicited with the EQ-5D-5L, in which the median utility for subjects aged 65–74 years was 0.90, which overlaps with the median age of prostate cancer diagnosis, 67 years [48, 49]. Utilities for local, regional, and distant disease were based on values ascertained from a subject pool of men in the US aged 60 and older (52% having been diagnosed with prostate cancer), using a computer-based utility assessment program designed to elicit utility values for health states related to prostate cancer using a standard gamble task [50]. Utilities for erectile dysfunction and urinary incontinence were based on a cost-utility analysis of treatments for localized prostate cancer from a US payer perspective, which sourced utility values from the Tufts Medical Center Cost-Effectiveness Analysis Registry (CEAR) and validated them with an expert panel [29, 51]. The utility of death, either prostate cancer-related or by other causes, was assumed to be zero. An annual discount rate of 3% was applied, in accordance with guidance for US-based studies [46].

2.6 Analyses

The outcomes of total healthcare costs, life-years (LY), and QALYs associated with each of the alternative imaging strategies were assessed. The incremental cost-effectiveness ratio (ICER) was calculated using the cost difference between two strategies, divided by the difference in QALYs. A strategy was considered cost effective relative to another strategy if the ICER was lower than a willingness-to pay (WTP) threshold of $150,000 USD per QALY. This WTP threshold of $150,000 was consistent with the upper range used as the standard for health-benefit price benchmarks by the Institute for Clinical and Economic Review [52]. The net monetary benefit of a given strategy was calculated by multiplying the WTP threshold by the total QALYs gained from using the strategy, then subtracting the total cost of the strategy.

2.6.1 Deterministic Sensitivity Analyses (DSA)

In addition to the base-case analyses, DSA were conducted that varied the following parameters: starting PSA distribution for each true disease status; the sensitivity and specificity of the diagnostics; the cost of the diagnostics; the disease distribution of local, regional, and distant disease; the utilities of the disease states; and the probability of therapeutic cure at initial diagnosis from local and regional disease for all treatment options. All parameters were varied to match the lower and upper limits, respectively, of the 95% confidence intervals as determined by the parametric distributions used in the probability sensitivity analyses.

2.6.2 Probabilistic Sensitivity Analyses

Probabilistic sensitivity analyses were conducted in Excel to estimate uncertainty of the base-case results. A beta distribution was assigned for binary variables (test performance, utilities, transition probabilities in the Markov model, and cure probabilities), a gamma distribution was assigned to cost parameters, and a Dirichlet distribution was assigned for true disease distribution. The number of iterations was set to 500, based on convergences plots of the ICER when comparing piflufolastat F 18 with fluciclovine F 18, PSMA 11, and SOC imaging (i.e., CT, MRI, and SPECT) (Fig. S2). The variables were varied based on the standard error (SE) if available, or SE calculated from the confidence intervals if available; if the SE or confidence intervals were not available, and the parameter was a proportion (p), then SE would be estimated using sample size (N) using $\sqrt{p * \frac{1-p}{N}}$; otherwise, SEs were assumed to be 15% of the mean (See Table S1 in the electronic supplementary material [ESM] for sources and values.)

2.7 Model Validation

The methods and reporting are consistent with the Consolidated Health Economic Evaluation Reporting Standards (CHEERS) checklist [53] (Table S3, see ESM). Clinical experts (see Acknowledgements) reviewed the assumptions, model structure, and results. Extreme value testing was conducted for the following variable categories: disease state

distribution, PSA distribution, test performance, treatment assignment, costs of diagnostics, transition probabilities, AE incidence rates, AE costs, impact of treatment (hazard rates), overall treatment costs, utilities, probability of curative therapy, and transition probabilities. Two versions of the core state transition model were coded independently in Excel to ensure that it was free of errors. Independent checks were done in the remaining Excel sheets to detect errors in formulas, and in Visual Basic for Applications (VBA) code to detect coding or logic errors.

3 Results

3.1 Base Case

Over a lifetime horizon, piflufolastat F 18 was predicted to have the greatest effectiveness in terms of LYs (6.80) and QALYs (5.33) among all the options compared. The associated LYs among the comparators ranged from 6.58 (SOC) to 6.76 (Ga68-PSMA 11), while QALYs ranged from 5.12 (SOC) to 5.30 (PSMA 11) (Table 4). Piflufolastat F 18 was also the most cost-effective option compared with fluciclovine F 18, PSMA 11, and SOC, with ICERs of $21,122, $55,836, and $124,330 per QALY gained, respectively, and extendedly dominated PSMA 11 and fluciclovine F 18. Despite having the highest cost ($172,235), piflufolastat F 18 was associated with the greatest net monetary benefit (NMB: $627,918) compared with fluciclovine F 18 (cost: $170,413 NMB: $618,933), PSMA 11 (cost: $169,810, NMB: $625,222), and SOC imaging (cost: $144,378, NMB: $623,421) at a WTP threshold of $150,000 (Table 4).

3.2 DSA

The DSA, which varied estimates of key drivers according to 95% confidence intervals, indicated that the common key drivers across all comparators included the cost of diagnostics, sensitivity of the tests, and utility value of no disease (Fig. S1, see ESM). The order of key drivers varied with the comparator chosen, but the top ten most influential factors were consistent across the comparators. The impact of the drivers on the ICER varied across comparators, although the ICERs were within the WTP threshold of $150,000 for the majority of scenarios.

3.2.1 Piflufolastat F 18 versus Fluciclovine F 18

Piflufolastat F 18 would dominate fluciclovine F 18 if the cost of piflufolastat F 18 was reduced by 26%, resulting in a lower incremental cost (− $5943) as well as higher QALYs gained (0.072) (Fig. S1a, see ESM). Similarly, piflufolastat F 18 would dominate fluciclovine F 18 when the latter's cost was increased by 32%. Except for these piflufolastat F 18-dominant scenarios, the ICERs of the DSA against fluciclovine F 18 ranged from $12,511 to $157,018 per QALY, with none of the scenarios have an ICER above a WTP threshold of $150,000. Therefore, piflufolastat F 18 remained cost effective compared with fluciclovine F 18.

3.2.2 Piflufolastat F 18 versus Ga68-PSMA-11

Similar to the comparison with fluciclovine F 18, piflufolastat F 18 would dominate PSMA 11 if its cost was reduced by 26% or the cost of PSMA 11 increased by 32% (Fig. S1b, see ESM). Besides costs, the most influential factor in this

Table 4 Cost-effectiveness base-case results

Diagnostic options	Total			Incremental outcomes (piflufolastat F 18 vs each comparator)			Combined outcomes		
	Cost (USD)	LY	QALY	Δ Cost (USD)	Δ LY	Δ QALY	ICER (Δ $/Δ LY)	ICER (Δ $/Δ QALY)	Net monetary benefit (threshold of $150,000)
Piflufolastat F 18	172,235	6.80	5.334						627,918
Comparators									
Fluciclovine F 18	170,413	6.72	5.262	1822	0.0863	0.0720	21,122	25,288	618,933
PSMA 11	169,810	6.76	5.300	2425	0.0434	0.0341	55,836	71,032	625,222
SOC imaging (MRI, SPECT, CT equally weighted)	144,378	6.58	5.119	27,857	0.2241	0.2157	124,330	129,151	623,421

Costs are presented in 2021 United States dollars (USD)

CT computed tomography, *ICER* incremental cost-effectiveness ratio, *LY* life-year, *MRI* magnetic resonance imaging, *PSMA* prostate-specific membrane antigen, *QALY* quality-adjusted life-year, *SOC* standard of care, *SPECT* single-photon emission computerized tomography

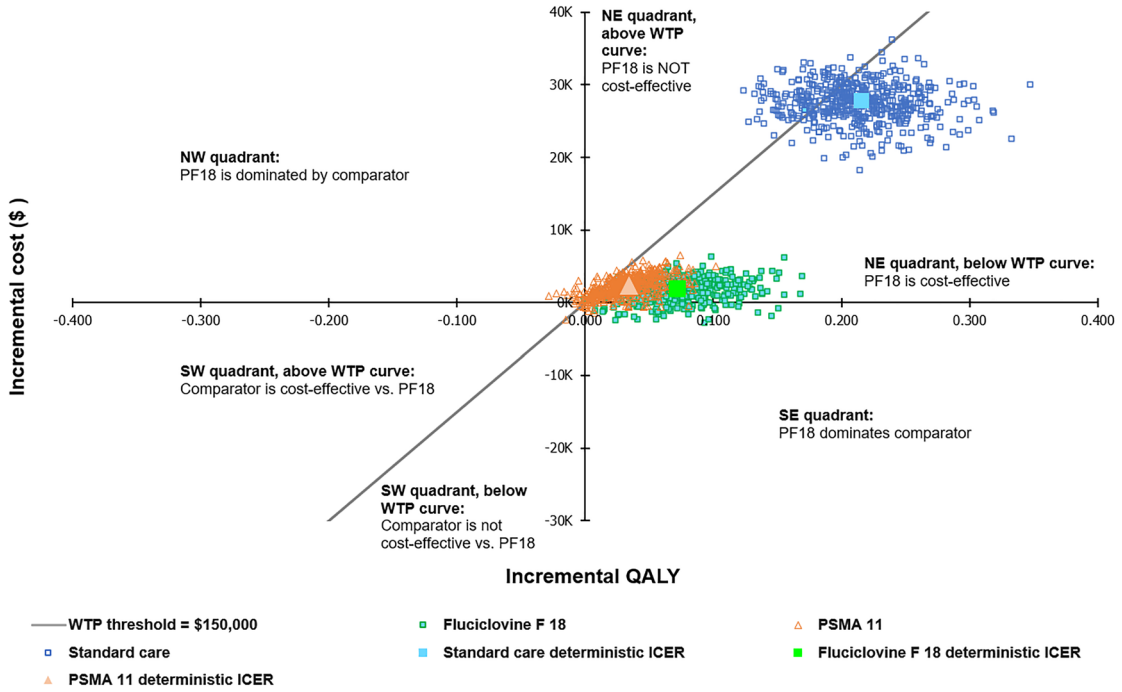

Fig. 2 Cost-effectiveness plane for piflufolastat F 18 vs all comparators. Costs are presented in 2021 United States dollars. *ICER* incremental cost-effectiveness ratio, *NE* northeast, *NW* northwest, *PSMA 11* gallium Ga68 PSMA-11, *SE* southeast, *SW* southwest, *WTP* willingness to pay

comparison was the sensitivity of the imaging modalities among the populations with PSA ≥1.0. The ICER of piflufolastat F 18 versus PSMA 11 would increase to $134,156 per QALY with a 4% reduced sensitivity of piflufolastat F 18, or to $272,432 per QALY with a 12% increased sensitivity for PSMA 11. The ICERs in the other scenarios are all under the WTP threshold of $150,000.

3.2.3 Piflufolastat F 18 versus Standard of Care Imaging (CT, MRI, SPECT)

In the comparison of piflufolastat F 18 versus SOC imaging, the most influential factor was the utility of the no disease (prostate cancer) state (Fig. S1c, see ESM). When reducing the utility of no disease state from 0.9 in the base case to 0.79 (which happens to be equal to the base case utility of local prostate cancer), the ICER increased to $167,630 per QALY. In the remaining scenarios, there was little impact on ICERs, which were all within the WTP threshold of $150,000.

3.3 Probabilistic Sensitivity Analysis

With approximately 350 simulations, the probabilistic ICER becomes stable based on visual inspection (see ICER convergence plot in Fig. S2, see ESM). A total of 500 simulations were run for the probabilistic analysis. The results of the probabilistic sensitivity analysis were similar to those of the base case, with piflufolastat F 18 providing the highest number of LYs (6.82) and QALYs (5.35), as well as the highest net monetary benefit ($630,374), versus the other comparators (Table S2, see ESM).

3.4 Cost-Effectiveness Plane

The cost-effectiveness plane and cost-effectiveness curve for piflufolastat F 18 versus the comparators are illustrated in Figs. 2 and 3, respectively. When comparing piflufolastat F 18 with fluciclovine F 18 or PSMA 11 on the cost-effectiveness plane, the ICER fell in the northeast quadrant, under the $150,000 WTP threshold, in a majority of the simulations (Fig. 2). However, there were some uncertainties in both incremental costs and QALYs (simulated incremental cost and QALYs are on both sides of the axes). When comparing piflufolastat F 18 with SOC imaging on the cost-effectiveness plane, piflufolastat F 18 was associated with higher costs in all simulations, although a greater magnitude of incremental benefit was also observed in the majority of the simulations.

The probability that piflufolastat F 18 is cost effective at a WTP threshold of $150,000 was 99.6% compared with fluciclovine F 18, 86.0% compared with PSMA 11, and 75.8% compared with SOC imaging, respectively. Alone, the probability of being cost effective at a WTP threshold was 66.6% for piflufolastat F 18, 0.0% for fluciclovine F 18, 9.6% for PSMA 11, and 23.8% for SOC imaging (Fig. 3).

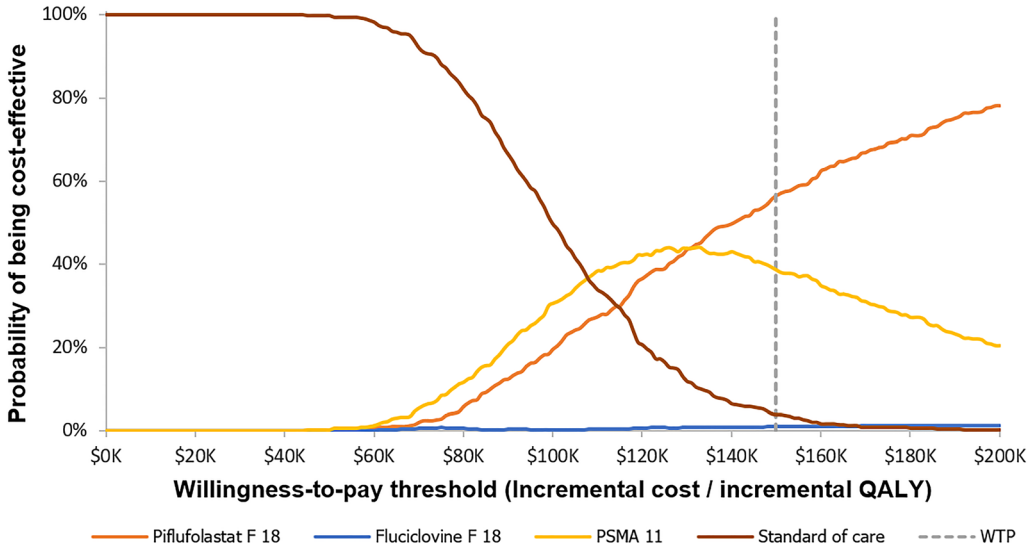

Fig. 3 Cost-effectiveness acceptability curve (combined). *PSMA* prostate-specific membrane antigen, *QALY* quality-adjusted life-year, *WTP* willingness to pay

4 Discussion

Accurate staging at initial prostate cancer diagnosis and detection and localization of BCR are critical for guiding disease management and treatment decisions. With the advent of novel PET radiotracers, evidence on the relative cost effectiveness of newer versus conventional imaging modalities is needed for optimal prostate cancer care and healthcare resource allocation.

In the current study's model, piflufolastat F 18 was found to be a cost-effective prostate cancer imaging option for use in the initial diagnostic workup and in the detection of BCR, compared with existing alternatives within the US health system. Although piflufolastat F 18 had a greater total cost than its comparators over a lifetime horizon, it was expected to lead to the greatest benefits in both LYs and QALYs. The model's results were sensitive to diagnostic cost, diagnostic sensitivity, regional/distant disease distribution, starting PSA distribution, and the utilities of having no disease or local disease. Despite greater uncertainties in the ICER of piflufolastat F 18 versus PSMA 11 compared with that of piflufolastat F 18 versus fluciclovine F 18 or SOC imaging, primarily due to uncertainty in the incremental QALYs, piflufolastat F 18 still had a slightly higher likelihood of being more cost effective than PSMA 11 (58%) at a WTP threshold of $150,000 per QALY gained. This is likely driven by the higher sensitivity (for PSA ≤1.0 and PSA >1.0) and specificity (only for PSA ≤ 1.0) of piflufolastat F 18 relative to PSMA 11 found in input sources, despite the fact that both are PSMA-targeting agents. Collectively, the current study model suggests that piflufolastat F 18 is more cost effective than the SOC imaging for prostate cancer, and the results were robust to a variety of scenarios in the DSA and PSA.

The total costs of newer imaging techniques are generally expected to be higher compared with conventional imaging modalities such as MRI, CT, or SPECT, as reflected in the current analysis. Nonetheless, the improved diagnostic performance of the newer techniques may provide improved clinical benefits, rendering them a more cost-effective option. In fact, prostate cancer management guidelines have recognized that PSMA PET is an effective imaging tool and advise that no other imaging tests would be necessary during initial prostate cancer diagnosis or at BCR.

Previous studies in different healthcare settings have suggested that novel PET radiotracers could be more cost effective or could improve clinical management of prostate cancer compared with conventional imaging. For example, a cost-effectiveness analysis from the Australian health system perspective evaluated PSMA 11 PET/MRI versus usual care (MRI and bone scan) among 30 patients with BCR prostate cancer using data from a prospective, single-center, single-arm study [54]. It found that, over a 10-year horizon, a diagnostic strategy with PSMA 11 was expected to produce 7.48 LY compared with 7.41 LY with usual care (QALYs were not assessed), and that PSMA 11 had an 87% higher likelihood of being cost effective at acceptable WTP thresholds. Another study based in Australia found that PSMA PET/CT compared with CT + whole body bone scan had an estimated 91% probability of being cost effective at a threshold of $50,000 AUD/QALY gained [55]. Notably, the ICER for this comparison was $21,147 AUD, a lower level than the comparable ICER found in the current study ($124,330 USD). This may have been primarily driven by

the higher estimated relative cost of PSMA PET compared with SOC treatment in Australia (~ 20% greater) versus the US (~800% greater). Additionally, a US cost-consequence study of fluciclovine F 18 based on a hypothetical hospital system serving 500,000 individuals used clinical inputs from the multicenter trial LOCATE (ClinicalTrials.org identifier: NCT0680041) [22]. That model estimated that, despite the higher total healthcare costs when including fluciclovine F 18 as an imaging modality for diagnosing and staging recurrent prostate cancer, there would be a 49.2% reduction in post-diagnosis management costs per correct diagnosis over 5 years. Further, the use of fluciclovine F18 was estimated to reduce unnecessary treatments by 19.2%. Another cost-effectiveness analysis of imaging modalities for detecting bone metastasis at BCR in France reported that PET imaging with 18F-choline was more cost effective than conventional MRI and PET [56].

Expanding on the literature, this study is the first of its kind to report that piflufolastat F 18 is not only more cost effective than SOC imaging but is also more cost effective relative to other PET tracers including PSMA 11 and fluciclovine F 18, both at initial and BCR prostate cancer diagnoses (notably, initial staging is not an indication for fluciclovine F 18). These findings may help inform US healthcare providers and payers on the clinical and economic value of piflufolastat F 18 as a diagnostic tool for prostate cancer.

The current model benefits from several strengths, including the ability to capture a relatively complete diagnostic management pathway starting from initial diagnosis to BCR, which is uncommon in previous cost-effectiveness models in prostate cancer [54, 56, 57]. In addition, a wide range of alternative diagnostics were incorporated into the model, with sensitivity and specificity of the diagnostic tests stratified by PSA to minimize the impact of different imaging test performances owing to different PSA levels [9, 58]. Furthermore, a wide range of treatments were modeled and the associated costs and disutilities of treatment-related AEs were included, which captured the relative cost savings and benefits from avoiding unnecessary treatments among patients unlikely to benefit from them.

The FDA approval of PSMA-PET imaging modalities has allowed for the incorporation of them into prostate cancer management guidelines. As clinicians increase their use of these for initial staging and follow-up imaging for disease recurrence, long-term outcomes will become available for real-world patients. The modeling in this study suggests that patients evaluated using PSMA-PET imaging will experience long-term benefits.

4.1 Limitations

This study is subject to certain limitations, some of which are common to economic evaluations. First, the sensitivity and specificity of piflufolastat F 18, as well as disease state and PSA level distributions among patients with prostate cancer, were based on values from the OSPREY and CONDOR clinical trials. Thus, these values may not be generalizable to the broader patient population with prostate cancer. Nonetheless, these parameters were tested in the DSA to evaluate the robustness of the base-case findings, and the resulting ICERs were found to be within the WTP threshold in a majority of the scenarios. Second, assumptions were made for treatment assignments based on the diagnosis of a particular disease state. Without a detailed analysis of claims data or medical records, it is not feasible to obtain accurate estimates of the proportion of patients with a given diagnosis who received a particular treatment. Thus, assumptions were informed by interviews with oncologists who treat prostate cancer in US clinical practice. Third, as a simplifying assumption, BCR could only occur once in the model, despite the possibility in the real world for patients to experience BCR more than once. Fourth, the model does not include chemotherapy among the first-line treatment options in either time point. Fifth, for some comparators, the sensitivity and specificity inputs were obtained from different sources, and using single arms from several studies. These were effectively naïve indirect comparisons, and therefore the differences in testing accuracy may be due to other confounding factors such as patient characteristics. Moreover, the sensitivity and specificity inputs overall were not specific to local, regional, or metastatic disease, but rather varied according to PSA levels. Sixth, a recent systematic review and meta-analysis found different values for test accuracy compared with the current study, and moreover, found that the type of radiotracer was not a significant factor for accuracy; the same authors also found differences in ICER when comparing PSMA PET/CT with standard of care [19, 55]. The test accuracy values in the current study were obtained using a targeted literature review, which is limited in scope compared with a systematic review and meta-analysis. The differences in ICER could largely be attributed to differences in estimated cost ratios between PSMA PET/CT and standard of care in Australia versus the US, but it is nonetheless a limitation of the current study. Lastly, the model did not account for future changes in the costs of diagnostics or treatment.

5 Conclusions

The use of more accurate diagnostic imaging tools is essential for guiding treatment decisions in prostate cancer, which would be expected to improve the health outcomes of patients. Incorrect staging, particularly at the time of primary diagnosis, can lead to increased costs attributable to

repeat testing and suboptimal treatment pathways, in addition to adversely impacting survival and quality of life. This study suggests that piflufolastat F 18 is a cost-effective diagnostic option for prostate cancer patients in the US, and with higher associated LY, QALY, and greater net monetary benefit than fluciclovine F 18, PSMA 11, and SOC imaging.

Supplementary Information The online version contains supplementary material available at https://doi.org/10.1007/s40273-023-01322-2.

Acknowledgements The authors thank Dr Daniel Lin, MD, of the University of Washington School of Medicine; Dr Edward Schaeffer, MD, PhD, of Northwestern University; Dr Eric Klein, MD, of the Cleveland Clinic; Dr Soroush Rais-Bahrami, MD, MBA, of the University of Alabama at Birmingham; and Dr Bela Denes, MD, of Lantheus, for providing their helpful insights on clinical inputs and study design. Medical writing was provided by Shelley Batts, PhD, an independent contractor of Analysis Group, Inc., and funded by Lantheus.

Declarations

Funding The study, manuscript preparation, and Open Access fee were funded by Lantheus.

Conflicts of interest Christopher Yee, Yiqiao Xin, and Noam Kirson are employees of Analysis Group, Inc., which has received consulting fees from Lantheus; Michael Harvey was an employee of Analysis Group, Inc. at the time of the study's conduct.

Availability of data and material Data and material will be made available on reasonable request.

Ethics approval Not applicable.

Consent to participate Not applicable.

Consent for publication Not applicable.

Code availability Not applicable.

Author contributions All authors were involved in the conceptualization and design of the study. CY, MH, and YX procured and prepared the data and conducted the analyses. Manuscript drafts were developed with input from all authors with the assistance of a professional medical writer. All authors have read and approved the final version of the manuscript.

References

1. Eastham JA, Auffenberg GB, Barocas DA, Chou R, Crispino T, Davis JW, et al. Clinically localized prostate cancer: AUA/ASTRO guideline, part I: introduction, risk assessment, staging, and risk-based management. J Urol. 2022;208(1):10–8.
2. National Cancer Institute: SEER. Cancer Stat Facts: Prostate Cancer. 2022. https://seer.cancer.gov/statfacts/html/prost.html. Accessed June 23.
3. Siegel RL, Miller KD, Fuchs HE, Jemal A. Cancer statistics, 2022. CA Cancer J Clin. 2022;72(1):7–33.
4. Artibani W, Porcaro AB, De Marco V, Cerruto MA, Siracusano S. Management of biochemical recurrence after primary curative treatment for prostate cancer: a review. Urol Int. 2018;100(3):251–62.
5. Briganti A, Joniau S, Gandaglia G, Cozzarini C, Sun M, Tombal B, et al. Patterns and predictors of early biochemical recurrence after radical prostatectomy and adjuvant radiation therapy in men with pT3N0 prostate cancer: implications for multimodal therapies. Int J Radiat Oncol Biol Phys. 2013;87(5):960–7.
6. Rebello RJ, Oing C, Knudsen KE, Loeb S, Johnson DC, Reiter RE, et al. Prostate cancer. Nat Rev Dis Primers. 2021;7(1):9.
7. Bednarova S, Lindenberg ML, Vinsensia M, Zuiani C, Choyke PL, Turkbey B. Positron emission tomography (PET) in primary prostate cancer staging and risk assessment. Transl Androl Urol. 2017;6(3):413–23.
8. Eastham JA, Auffenberg GB, Barocas DA, Chou R, Crispino T, Davis JW, et al. Clinically localized prostate cancer: AUA/ASTRO guideline, part II: principles of active surveillance, principles of surgery, and follow-up. J Urol. 2022;208(1):19–25.
9. Fendler WP, Calais J, Eiber M, Flavell RR, Mishoe A, Feng FY, et al. Assessment of 68Ga-PSMA-11 PET accuracy in localizing recurrent prostate cancer: a prospective single-arm clinical trial. JAMA Oncol. 2019;5(6):856–63.
10. FDA approves second PSMA-targeted PET imaging drug formen with prostate cancer [press release]. 2021.
11. De Visschere PJL, Standaert C, Futterer JJ, Villeirs GM, Panebianco V, Walz J, et al. A systematic review on the role of imaging in early recurrent prostate cancer. Eur Urol Oncol. 2019;2(1):47–76.
12. Lowrance WT, Breau RH, Chou R, Chapin BF, Crispino T, Dreicer R, et al. Advanced prostate cancer: AUA/ASTRO/SUO guideline part II. J Urol. 2021;205(1):22–9.
13. Meijer D, Eppinga WSC, Mohede RM, Vanneste BGL, Meijnen P, Meijer OWM, et al. Prostate-specific membrane antigen positron emission tomography/computed tomography is associated with improved oncological outcome in men treated with salvage radiation therapy for biochemically recurrent prostate cancer. Eur Urol Oncol. 2022;5(2):146–52.
14. Lowrance WT, Breau RH, Chou R, Chapin BF, Crispino T, Dreicer R, et al. Advanced prostate cancer: AUA/ASTRO/SUO guideline part I. J Urol. 2021;205(1):14–21.
15. Morris MJ, Rowe SP, Gorin MA, Saperstein L, Pouliot F, Josephson D, et al. Diagnostic performance of (18)F-DCFPyL-PET/CT in men with biochemically recurrent prostate cancer: results from the condor phase iii, multicenter study. Clin Cancer Res. 2021;27(13):3674–82.
16. Rousseau E, Wilson D, Lacroix-Poisson F, Krauze A, Chi K, Gleave M, et al. A prospective study on (18)F-DCFPyL PSMA PET/CT imaging in biochemical recurrence of prostate cancer. J Nucl Med. 2019;60(11):1587–93.
17. Pouliot F, Carroll P, Probst S, Pienta KJ, Rowe SP, Saperstein L, et al. A prospective phase II/III multicenter study of PSMA-targeted 18F-DCFPyL PET/CT imaging in patients with prostate cancer (OSPREY): A sub-analysis of regional and distant

metastases detection rates at initial staging by 18F-DCFPyL PET/CT. J Clin Oncol. 2020;38:9.
18. Pienta KJ, Gorin MA, Rowe SP, Carroll PR, Pouliot F, Probst S, et al. A phase 2/3 prospective multicenter study of the diagnostic accuracy of prostate specific membrane antigen PET/CT with (18)F-DCFPyL in prostate cancer patients (OSPREY). J Urol. 2021;206(1):52–61.
19. Jeet V, Parkinson B, Song R, Sharma R, Hoyle M. Histopathologically validated diagnostic accuracy of PSMA-PET/CT in the primary and secondary staging of prostate cancer and the impact of PSMA-PET/CT on clinical management: a systematic review and meta-analysis. Semin Nucl Med. 2023;53(5):706–18.
20. Progenics. Clinical Study Report: PyL-2301. 2020.
21. Progenics. Clinical Study Report: PyL-3301. 2020.
22. Jensen IS, Hathway J, Cyr P, Gauden D, Gardiner P. Cost-consequence analysis of (18)F-fluciclovine for the staging of recurrent prostate cancer. J Mark Access Health Policy. 2020;8(1):1749362.
23. Andriole GL, Kostakoglu L, Chau A, Duan F, Mahmood U, Mankoff DA, et al. The impact of positron emission tomography with 18F-fluciclovine on the treatment of biochemical recurrence of prostate cancer: results from the LOCATE trial. J Urol. 2019;201(2):322–31.
24. Cowen ME, Chartrand M, Weitzel WF. A Markov model of the natural history of prostate cancer. J Clin Epidemiol. 1994;47(1):3–21.
25. de Koning HJ, Auvinen A, Berenguer-Sanchez A, Calais-da-Silva F, Ciatto S, Denis L, et al. Large-scale randomized prostate cancer screening trials: program performances in the European Randomized Screening for Prostate Cancer trial and the Prostate, Lung, Colorectal and Ovary cancer trial. Int J Cancer. 2002;97(2):237–44.
26. de Koning HJ, Liem MK, Baan CA, Boer R, Schroder FH, Alexander FE, et al. Prostate cancer mortality reduction by screening: power and time frame with complete enrollment in the European Randomised Screening for Prostate Cancer (ERSPC) trial. Int J Cancer. 2002;98(2):268–73.
27. Draisma G, Boer R, Otto SJ, van der Cruijsen IW, Damhuis RA, Schroder FH, et al. Lead times and overdetection due to prostate-specific antigen screening: estimates from the European Randomized Study of Screening for Prostate Cancer. J Natl Cancer Inst. 2003;95(12):868–78.
28. Young JL Jr, Percy CL, Asire AJ, Berg JW, Cusano MM, Gloeckler LA, et al. Cancer incidence and mortality in the United States, 1973–77. Natl Cancer Inst Monogr. 1981;57:1–187.
29. Cooperberg MR, Ramakrishna NR, Duff SB, Hughes KE, Sadownik S, Smith JA, et al. Primary treatments for clinically localised prostate cancer: a comprehensive lifetime cost-utility analysis. BJU Int. 2013;111(3):437–50.
30. Sciarra A, Fasulo A, Ciardi A, Petrangeli E, Gentilucci A, Maggi M, et al. A meta-analysis and systematic review of randomized controlled trials with degarelix versus gonadotropin-releasing hormone agonists for advanced prostate cancer. Med (Baltim). 2016;95(27):e3845.
31. Zhou JT, Fang DM, Xia S, Li T, Liu RL. The incidence proportion of erectile dysfunction in patients treated with cryotherapy for prostate cancer: a meta-analysis. Clin Transl Oncol. 2019;21(9):1152–8.
32. Roberts CB, Jang TL, Shao YH, Kabadi S, Moore DF, Lu-Yao GL. Treatment profile and complications associated with cryotherapy for localized prostate cancer: a population-based study. Prostate Cancer Prostatic Dis. 2011;14(4):313–9.
33. Trock BJ, Han M, Freedland SJ, Humphreys EB, DeWeese TL, Partin AW, et al. Prostate cancer-specific survival following salvage radiotherapy vs observation in men with biochemical recurrence after radical prostatectomy. JAMA. 2008;299(23):2760–9.
34. Bauman G, Ding K, Chin J, Nair S, Iaboni A, Crook J, et al. Cryosurgery versus primary androgen deprivation therapy for locally recurrent prostate cancer after primary radiotherapy: a propensity-matched survival analysis. Cureus. 2020;12(5):e7983.
35. Chade DC, Shariat SF, Cronin AM, Savage CJ, Karnes RJ, Blute ML, et al. Salvage radical prostatectomy for radiation-recurrent prostate cancer: a multi-institutional collaboration. Eur Urol. 2011;60(2):205–10.
36. Scarsbrook AF, Bottomley D, Teoh EJ, Bradley KM, Payne H, Afaq A, et al. Effect of (18)F-fluciclovine positron emission tomography on the management of patients with recurrence of prostate cancer: results from the FALCON Trial. Int J Radiat Oncol Biol Phys. 2020;107(2):316–24.
37. Bach-Gansmo T, Nanni C, Nieh PT, Zanoni L, Bogsrud TV, Sletten H, et al. Multisite experience of the safety, detection rate and diagnostic performance of fluciclovine ((18)F) positron emission tomography/computerized tomography imaging in the staging of biochemically recurrent prostate cancer. J Urol. 2017;197(3 Pt 1):676–83.
38. Asokendaran ME, Meyrick DP, Skelly LA, Lenzo NP, Henderson A. Gallium-68 prostate-specific membrane antigen positron emission tomography/computed tomography compared with diagnostic computed tomography in relapsed prostate cancer. World J Nucl Med. 2019;18(3):232–7.
39. de Leiris N, Leenhardt J, Boussat B, Montemagno C, Seiller A, Phan Sy O, et al. Does whole-body bone SPECT/CT provide additional diagnostic information over [18F]-FCH PET/CT for the detection of bone metastases in the setting of prostate cancer biochemical recurrence? Cancer Imaging. 2020;20(1):58.
40. Li Y, Han D, Wu P, Ren J, Ma S, Zhang J, et al. Comparison of (68)Ga-PSMA-617 PET/CT with mpMRI for the detection of PCa in patients with a PSA level of 4–20 ng/ml before the initial biopsy. Sci Rep. 2020;10(1):10963.
41. Centers for Medicare & Medicaid Services. Physician Fee Schedule. 2020. https://www.cms.gov/apps/physician-fee-schedule/search/search-criteria.aspx. Accessed Dec 2020.
42. RED BOOK Online. IBM Micromedex [Internet]. 2022. https://www.micromedexsolutions.com.
43. Research Data Assistance Center (ResDac). 2018. https://www.resdac.org/. Accessed 21 Aug 2018.
44. Appukkuttan S, Tangirala K, Babajanyan S, Wen L, Simmons S, Shore N. A retrospective claims analysis of advanced prostate cancer costs and resource use. Pharmacoecon Open. 2020;4(3):439–47.
45. Tangirala K, Appukkuttan S, Simmons S. Costs and healthcare resource utilization associated with hospital admissions of patients with metastatic or nonmetastatic prostate cancer. Am Health Drug Benefits. 2019;12(6):306–12.
46. Haacker M, Hallett TB, Atun R. On discount rates for economic evaluations in global health. Health Policy Plan. 2019;35(1):107–14.
47. U.S. Bureau of Labor Statistics. Consumer Price Index—All Urban Consumers Not Seasonally Adjusted U.S. City Average for Medical care, 2000–2020. 2020. http://download.bls.gov/pub/time.series/cu/cu.data.15.USMedical. Accessed Dec 2020.
48. Jiang R, Janssen MFB, Pickard AS. US population norms for the EQ-5D-5L and comparison of norms from face-to-face and online samples. Qual Life Res. 2021;30(3):803–16.
49. National Cancer Institute S, Epidemiology, and End Results (SEER) Program. Cancer Stat Facts: Prostate Cancer. 2022. https://seer.cancer.gov/statfacts/html/prost.html.
50. Stewart ST, Lenert L, Bhatnagar V, Kaplan RM. Utilities for prostate cancer health states in men aged 60 and older. Med Care. 2005;43(4):347–55.
51. Center for the Evaluation of Value and Risk in Health. The Cost-Effectiveness Analysis Registry [Internet]. (Boston), Institute

for Clinical Research and Health Policy Studies, Tufts Medical Center. 2022. https://cear.tuftsmedicalcenter.org/.
52. Institute for Clinical and Economic Review (ICER). 2020-2023 Value Assessment Framework. 2020. https://icer.org/wp-content/uploads/2020/10/ICER_2020_2023_VAF_102220.pdf.
53. Husereau D, Drummond M, Petrou S, Carswell C, Moher D, Greenberg D, et al. Consolidated health economic evaluation reporting standards (CHEERS) statement. Value Health. 2013;16(2):e1-5.
54. Gordon LG, Elliott TM, Joshi A, Williams ED, Vela I. Exploratory cost-effectiveness analysis of (68)Gallium-PSMA PET/MRI-based imaging in patients with biochemical recurrence of prostate cancer. Clin Exp Metastasis. 2020;37(2):305–12.
55. Song R, Jeet V, Sharma R, Hoyle M, Parkinson B. Cost-effectiveness analysis of prostate-specific membrane antigen (PSMA) positron emission tomography/computed tomography (PET/CT) for the primary staging of prostate cancer in Australia. Pharmacoeconomics. 2022;40(8):807–21.
56. Gauthe M, Zarca K, Aveline C, Lecouvet F, Balogova S, Cussenot O, et al. Comparison of (18)F-sodium fluoride PET/CT, (18)F-fluorocholine PET/CT and diffusion-weighted MRI for the detection of bone metastases in recurrent prostate cancer: a cost-effectiveness analysis in France. BMC Med Imaging. 2020;20(1):25.
57. Keeney E, Thom H, Turner E, Martin RM, Morley J, Sanghera S. Systematic review of cost-effectiveness models in prostate cancer: Exploring new developments in testing and diagnosis. Value Health. 2022;25(1):133–46.
58. Hoffmann MA, Buchholz HG, Wieler HJ, Miederer M, Rosar F, Fischer N, et al. PSA and PSA kinetics thresholds for the presence of (68)Ga-PSMA-11 PET/CT-detectable lesions in patients with biochemical recurrent prostate cancer. Cancers (Basel). 2020;12:2.

Authors and Affiliations

Christopher W. Yee[1] · Michael J. Harvey[1] · Yiqiao Xin[1] · Noam Y. Kirson[1]

✉ Christopher W. Yee
Christopher.Yee@analysisgroup.com

[1] Analysis Group, Inc., Boston, MA, USA